Supplementary Materials

Mo-Si alloys studied by atomistic computer simulations using a novel machine-learning interatomic potential: Thermodynamics and interface phenomena

Dr. Olena Lenchuk Dr. Jochen Rohrer Prof. Dr. Karsten Albe

Technical University Darmstadt, Institute of Materials Science, Otto-Berndt-Strasse 3, 64287 Darmstadt
Email Address: lenchuk@mm.tu-darmstadt.de

Keywords: *Machine-learning interatomic potential, Mo-Si alloys, refractory alloys, molecular dynamics*

1 Crystal structure of Mo-Si compounds

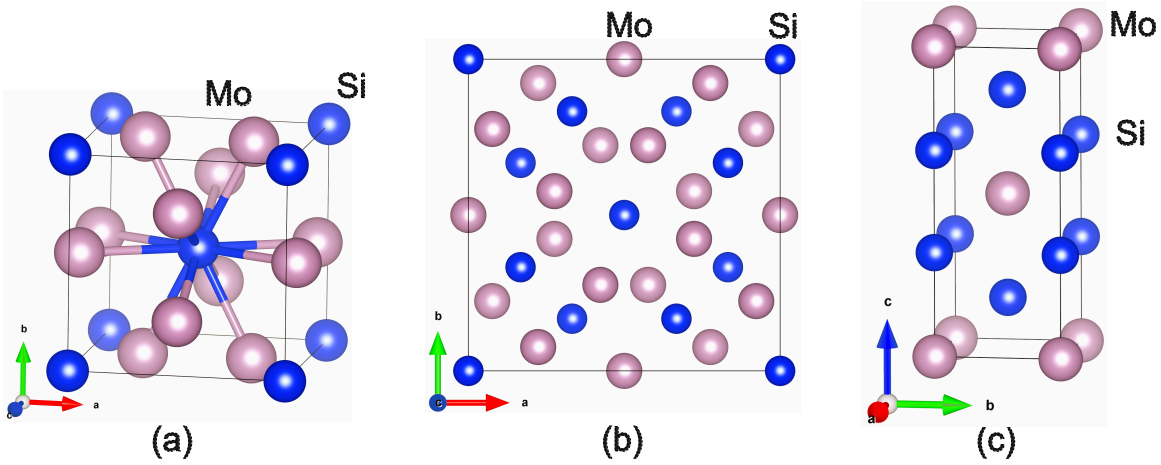

Figure S1: Crystal structure of (a) Mo_3Si, (b) Mo_5Si_3 and (c) $MoSi_2$ phases.

Figure S1 shows atomic structures of Mo_3Si, Mo_5Si_3 and $MoSi_2$ phases. The Mo_3Si phase has the cubic A15 (Cr_3Si type) structure, where the Si atoms occupy the bcc positions in the unit cell and the Mo atoms form three orthogonal chains along the [100], [010] and [001] directions on the cube faces [1]. Mo is bonded in a 6-coordinate geometry to two equivalent Mo and four equivalent Si atoms. Both Mo-Mo bond lengths are 2.44 Å. All Mo-Si bond lengths are 2.73 Å. Si is bonded to twelve equivalent Mo atoms to form a mixture of edge and face-sharing $SiMo_{12}$ cuboctahedra.

The Mo_5Si_3 phase has a complex body-centered tetragonal structure called the W_5Si_3-type structure with the space group of $I4/mcm$ (No.140). The crystal structure is characterized by two atomic chains of Mo-Mo and Si-Si atoms, extending along the c-axis with the bond length of 2.45 Å, which are believed to play a crutial role in determining thermal and elastic properties of Mo_5Si_3 phase [2, 3].

$MoSi_2$ crystallizes in the body-centered tetragonal $C11_b$ crystal structure (the spacegroup is $I4/mmm$), with two formula units in the unit cell [4]. Molybdenum atoms are surrounded by ten Si and four Mo atoms, while silicon atoms are surrounded by five Si and five Mo atoms, at different atomic distances.

2 Volume-energy curves of Mo, Si and Mo-Si phases

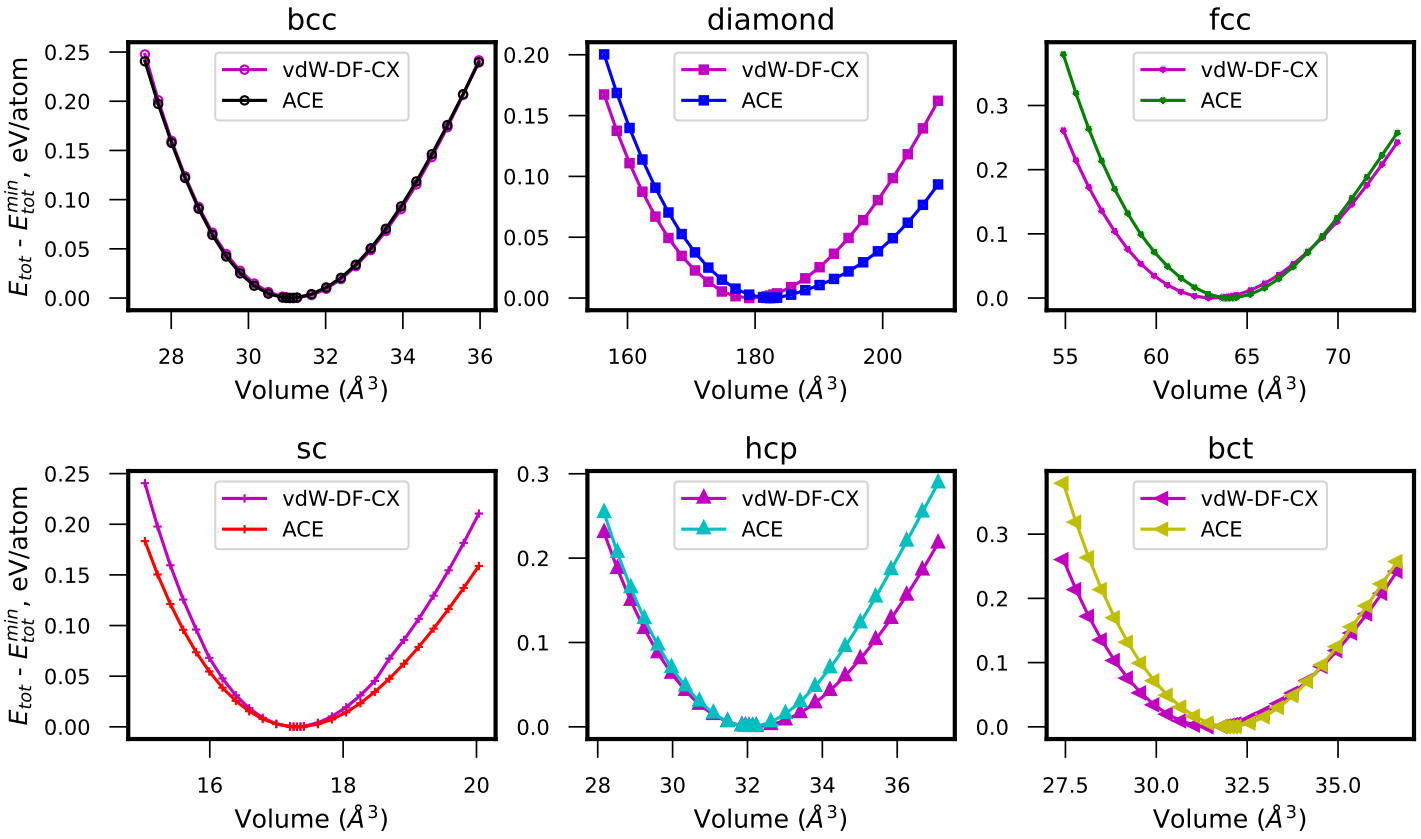

Figure S2: The energy-volume curves of Mo in different crystal structures, computed using ACE Mo-Si potential and vdW-DF-CX functional.

The cohesive energy E_{coh}, listed in Table S1, is computed according to

$$E_{\text{coh}} = E_{\text{tot}}(V) - E_{\text{tot}}^{\text{atom}}, \tag{1}$$

where $E_{\text{tot}}(V)$ is the total energy of the crystalline Mo computed for the various cell volumes V and $E_{\text{tot}}^{\text{atom}}$ is the total energy of the isolated atom. Note, that for the ACE potential, $E_{\text{tot}}^{\text{atom}} = 0$.

The formation energy E_{f}, listed in Table S2-Table S4 is computed as

$$E_{\text{f}} = E_{\text{tot}}(\text{Mo}_x\text{Si}_y) - x\epsilon_{\text{tot}}(\text{Mo}) - y\epsilon_{\text{tot}}(\text{Si}), \tag{2}$$

where $E_{\text{tot}}(\text{Mo}_x\text{Si}_y)$ is the total energy of the crystalline Mo_xSi_y compound, $\epsilon_{\text{tot}}(\text{Mo})$ and $\epsilon_{\text{tot}}(\text{Si})$ are the total energies of the bulk bcc Mo and bulk diamond Si (see Table S1).

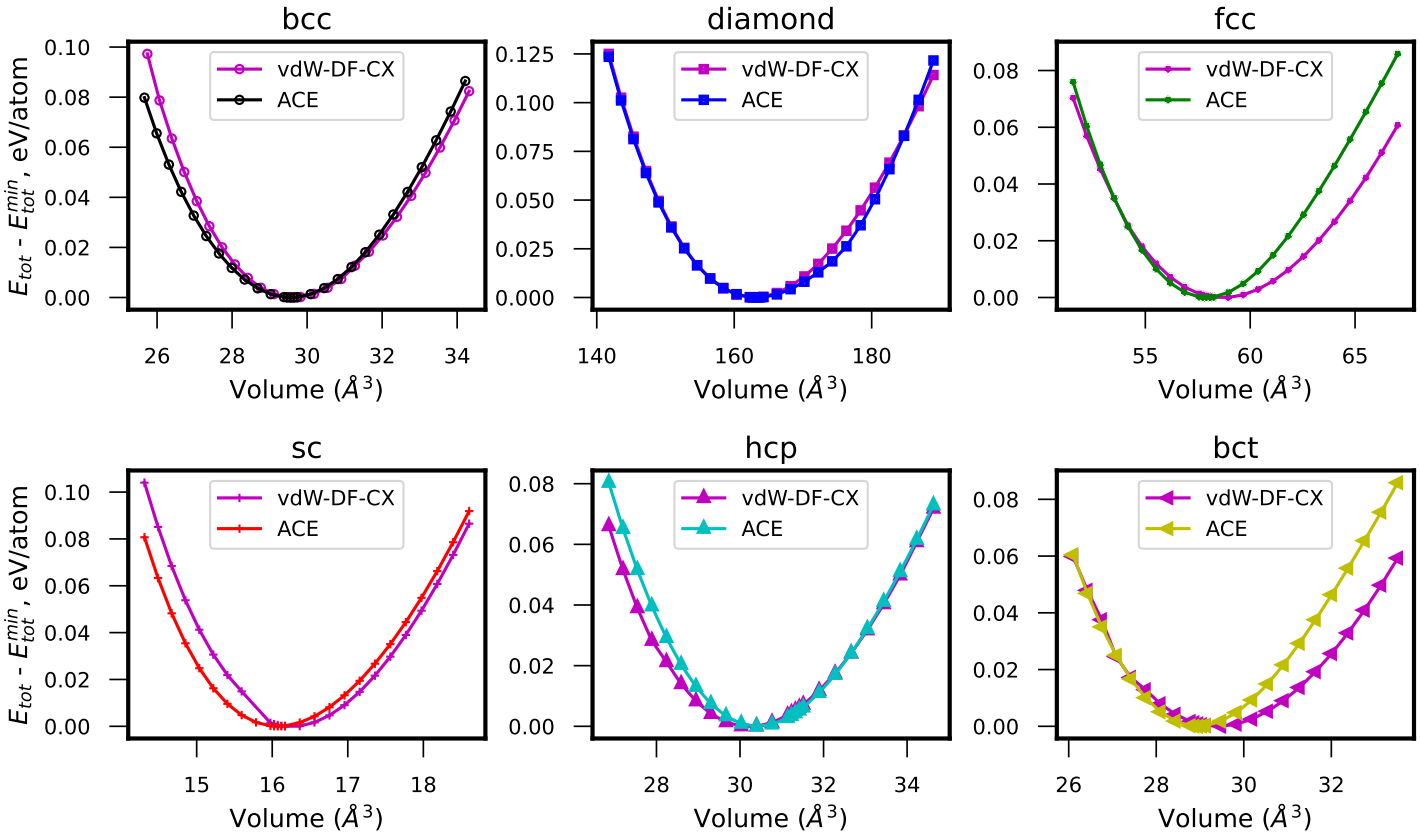

Figure S3: The energy-volume curves of Si in different crystal structures, computed using ACE Mo-Si potential and vdW-DF-CX functional.

	Mo			Si		
Structure	Lattice constant	Cohesive energy	Bulk modulus	Lattice constant	Cohesive energy	Bulk modulus
Mo-Si ACE						
bcc	3.14 Å	-7.05 eV/atom	264 GPa	3.09 Å	-4.42 eV/atom	88 GPa
diamond	5.67 Å	-4.73 eV/atom	92 GPa	5.47 Å	-4.88 eV/atom	93 GPa
fcc	4.00 Å	-6.76 eV/atom	299 GPa	3.87 Å	-4.43 eV/atom	107 GPa
sc	2.59 Å	-5.80 eV/atom	154 GPa	2.52 Å	-4.61 eV/atom	103 GPa
hcp	$a = b = 2.82$ Å, c=4.65 Å	-6.76 eV/atom	291 GPa	$a = b = 2.75$ Å, $c = 4.44$ Å	-4.43 eV/atom	103 GPa
bct	$a = b = 2.82$ Å, $c = 4.03$ Å	-6.76 eV/atom	299 GPa	$a = b = 2.74$ Å, $c = 3.87$ Å	-4.43 eV/atom	107 GPa
vdW-DF-CX						
bcc	3.15 Å	-7.05 eV/atom	267 GPa	3.09 Å	-4.42 eV/atom	94 GPa
diamond	5.64 Å	-4.70 eV/atom	113 GPa	5.46 Å	-4.89 eV/atom	91 GPa
fcc	3.98 Å	-6.63 eV/atom	246 GPa	3.89 Å	-4.40 eV/atom	83 GPa
sc	2.58 Å	-5.87 eV/atom	204 GPa	2.53 Å	-4.60 eV/atom	107 GPa
hcp	$a = b = 2.82$ Å, c= 4.65 Å	-6.57 eV/atom	236 GPa	$a = b = 2.79$ Å, $c = 4.51$ Å	-4.48 eV/atom	91 GPa
bct	$a = b = 2.80$ Å, $c = 4.00$ Å	-6.63 eV/atom	246 GPa	$a = b = 2.75$ Å, $c = 3.89$ Å	-4.40 eV/atom	83 GPa

Table S1: The lattice parameters, cohesive energies and bulk moduli of Mo and Si phases in different crystal structures, computed using ACE Mo-Si potential and vdW-DF-CX functional.

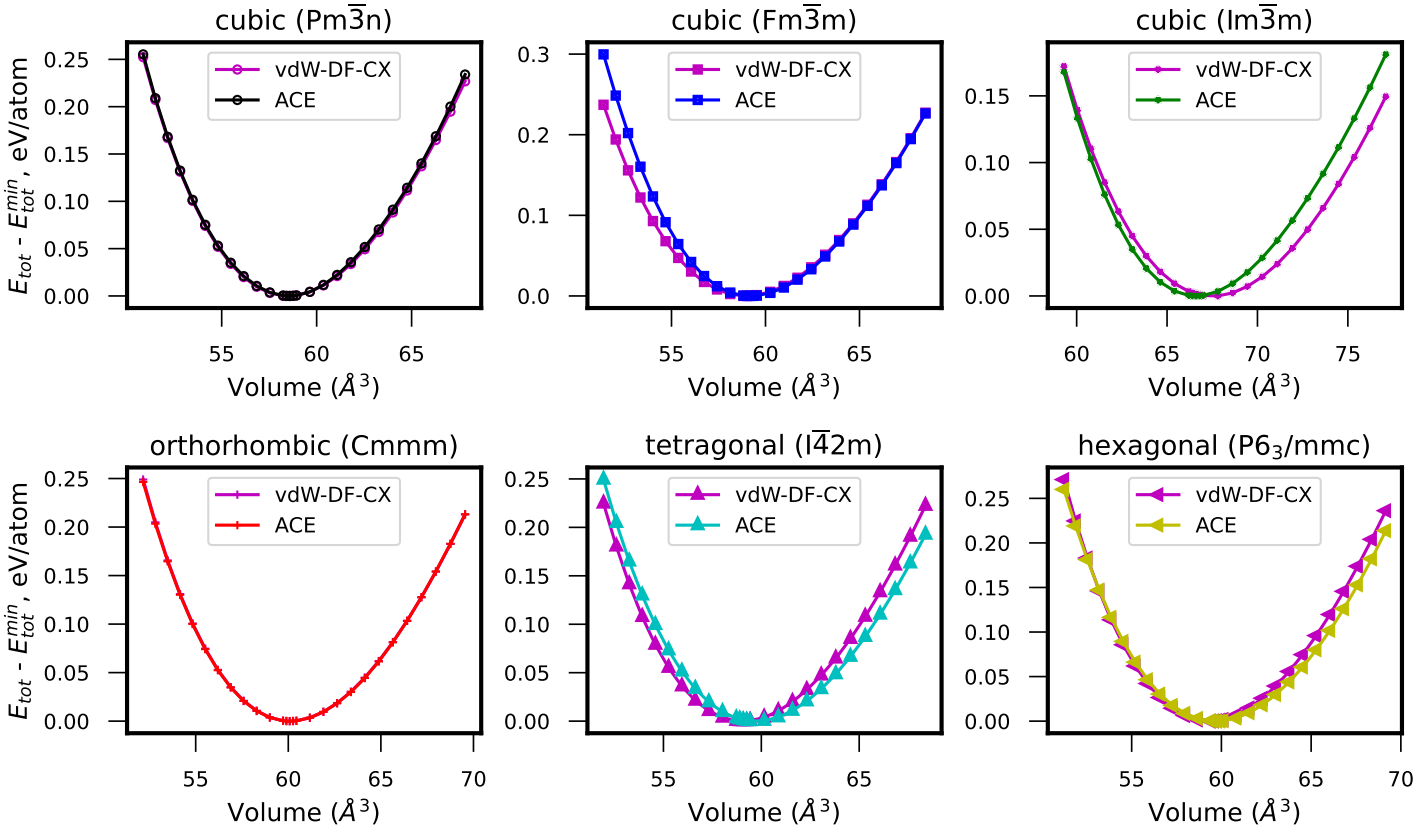

Figure S4: The energy-volume curves of Mo_3Si in different crystal structures, computed using ACE Mo-Si potential and vdW-DF-CX functional.

Mo_3Si					
Space group	Crystal System	Prototype	Lattice constant	Formation energy	Bulk modulus
Mo-Si ACE					
Pm$\bar{3}$n	cubic	Mo_3Si	$a = b = c = 4.89$ Å	-1.35 eV/stoich.unit	259 GPa
Fm$\bar{3}$m	cubic	Cr_3Ni	$a = b = c = 6.19$ Å	-0.65 eV/stoich.unit	273 GPa
Im$\bar{3}$m	cubic	V_3Si	$a = b = c = 5.11$ Å	+3.12 eV/stoich.unit	199 GPa
Cmmm	orthorhombic	V_3Ga	$a = 3.15$ Å, $b = 4.50$ Å, $c = 8.48$ Å	-0.06 eV/stoich.unit	237 GPa
I$\bar{4}$2m	tetragonal	V_3S	$a = b = 9.77$ Å, $c = 4.95$ Å	-0.93 eV/stoich.unit	260 GPa
P6$_3$/mmc	hexagonal	Cr_3Pt	$a = b = 5.54$ Å $c = 4.50$ Å	-0.24 eV/stoich.unit	225 GPa
vdW-DF-CX					
Pm$\bar{3}$n	cubic	Mo_3Si	$a = b = c = 4.89$ Å	-1.33 eV/stoich.unit	255 GPa
Fm$\bar{3}$m	cubic	Cr_3Ni	$a = b = c = 6.18$ Å	-0.30 eV/stoich.unit	246 GPa
Im$\bar{3}$m	cubic	V_3Si	$a = b = c = 5.14$ Å	+4.16 eV/stoich.unit	177 GPa
Cmmm	orthorhombic	V_3Ga	$a = 3.15$ Å, $b = 4.50$ Å, $c = 8.48$ Å	-0.08 eV/stoich.unit	238 GPa
I$\bar{4}$2m	tetragonal	V_3S	$a = b = 9.79$ Å, $c = 4.96$ Å	-0.87 eV/stoich.unit	249 GPa
P6$_3$/mmc	hexagonal	Cr_3Pt	$a = b = 5.53$ Å, $c = 4.49$ Å	-0.30 eV/stoich.unit	243 GPa

Table S2: The lattice parameters, formation energies and bulk moduli of Mo_3Si phase in different crystal structures, computed using ACE Mo-Si potential and vdW-DF-CX functional.

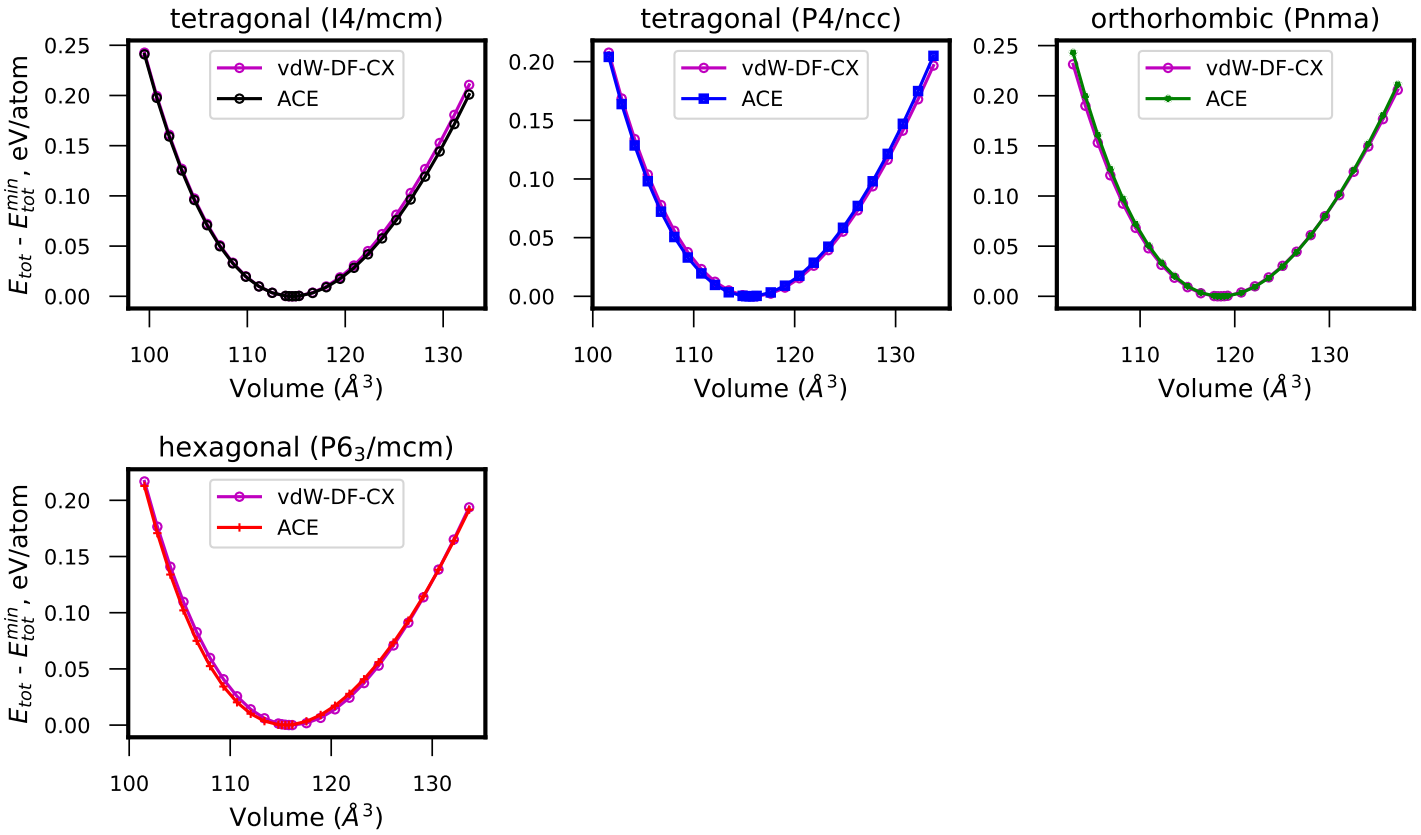

Figure S5: The energy-volume curves of Mo_5Si_3 in different crystal structures, computed using ACE Mo-Si potential and vdW-DF-CX functional.

Mo_5Si_3					
Space group	Crystal System	Prototype	Lattice constant	Formation energy	Bulk modulus
Mo-Si ACE					
I4/mcm	tetragonal	Mo_5Si_3	$a = b = 9.67$ Å, $c = 4.90$ Å	-3.30 eV/stoich.unit	238 GPa
P4/ncc	tetragonal	Ba_5Si_3	$a = b = 6.37$ Å, $c = 11.39$ Å	-2.51 eV/stoich.unit	243 GPa
Pnma	orthorhombic	Sr_5Bi_3	$a = 6.40$ Å, $b = 7.60$ Å, $c = 9.75$ Å	-2.15 eV/stoich.unit	237 GPa
P6$_3$/mcm	hexagonal	Mo_5Si_3	$a = b = 7.24$ Å, $c = 5.08$ Å	-2.21 eV/stoich.unit	241 GPa
vdW-DF-CX					
I4/mcm	tetragonal	Mo_5Si_3	$a = b = 9.67$ Å, $c = 4.90$ Å	-3.29 eV/stoich.unit	245 GPa
P4/ncc	tetragonal	Ba_5Si_3	$a = b = 6.38$ Å, $c = 11.40$ Å	-2.10 eV/stoich.unit	238 GPa
Pnma	orthorhombic	Sr_5Bi_3	$a = 6.40$ Å, $b = 7.60$ Å, $c = 9.75$ Å	-1.74 eV/stoich.unit	229 GPa
P6$_3$/mcm	hexagonal	Mo_5Si_3	$a = b = 7.26$ Å, $c = 5.09$ Å	-2.49 eV/stoich.unit	240 GPa

Table S3: The lattice parameters, formation energies and bulk moduli of Mo_5Si_3 phase in different crystal structures, computed using ACE Mo-Si potential and vdW-DF-CX functional.

$MoSi_2$					
Space group	Crystal System	Prototype	Lattice constant	Formation energy	Bulk modulus
Mo-Si ACE					
I4/mmm	tetragonal	$MoSi_2$	$a = b = 3.22$ Å, $c = 7.91$ Å	-1.54 eV/stoich.unit	208 GPa
$Fm\bar{3}m$	cubic	CaF_2	$a = b = c = 5.87$ Å	+0.73 eV/stoich.unit	161 GPa
$P6\_22\bar{2}$	hexagonal	$MoSi_2$	$a = b = 4.57$ Å, $c = 6.77$ Å,	-1.26 eV/stoich.unit	185 GPa
$Pmc2_1$	orthorhombic	CaF_2	$a = 3.24$ Å, $b = 4.72$ Å, $c = 5.93$ Å	+0.05 eV/stoich.unit	161 GPa
$P4_2/mnm$	tetragonal	TiO_2	$a = b = 6.33$ Å, $c = 2.83$ Å	+1.30 eV/stoich.unit	144 GPa
C2/m	monoclinic	TiO_2	$a = 11.07$ Å, $b = 4.33$ Å, $c = 7.64$ Å	-0.11 eV/stoich.unit	179 GPa
vdW-DF-CX					
I4/mmm	tetragonal	$MoSi_2$	$a = b = 3.21$ Å, $c = 7.91$ Å	-1.55 eV/stoich.unit	209 GPa
$Fm\bar{3}m$	cubic	CaF_2	$a = b = c = 5.86$ Å	+1.04 eV/stoich.unit	134 GPa
$P6\_22\bar{2}$	hexagonal	$MoSi_2$	$a = b = 4.56$ Å, $c = 6.76$ Å	-1.45 eV/stoich.unit	209 GPa
$Pmc2_1$	orthorhombic	CaF_2	$a = 3.26$ Å, $b = 4.75$ Å, $c = 5.97$ Å	+0.01 eV/stoich.unit	169 GPa
$P4_2/mnm$	tetragonal	TiO_2	$a = b = 6.37$ Å, $c = 2.84$ Å	+1.16 eV/stoich.unit	122 GPa
C2/m	monoclinic	TiO_2	$a = 11.07$ Å, $b = 4.33$ Å $c = 7.64$ Å	-0.23 eV/stoich.unit	179 GPa

Table S4: The lattice parameters, formation energies and bulk moduli of $MoSi_2$ phase in different crystal structures, computed using ACE Mo-Si potential and vdW-DF-CX functional.

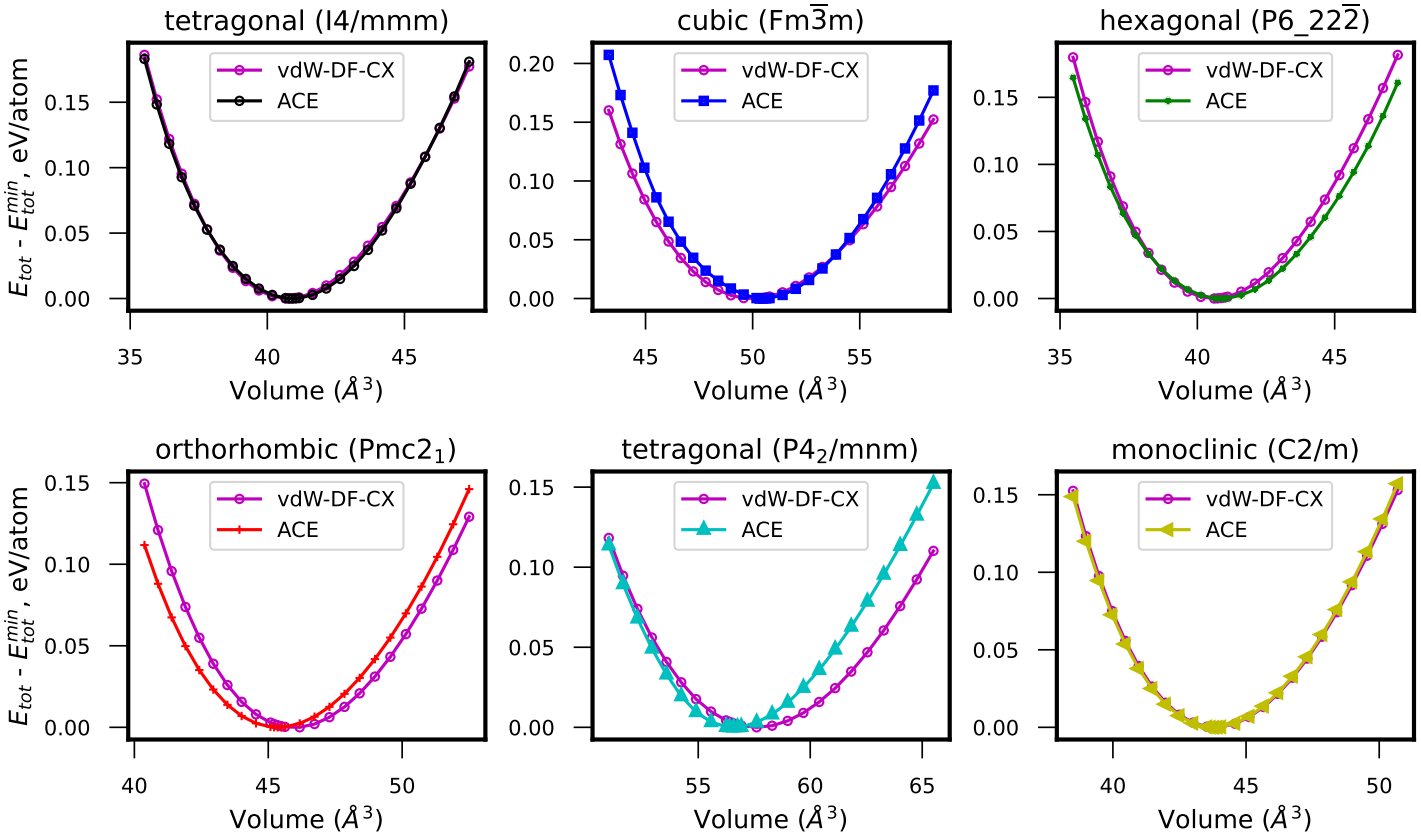

Figure S6: The energy-volume curves of $MoSi_2$ in different crystal structures, computed using ACE Mo-Si potential and vdW-DF-CX functional.

3 Enthalpy of formation

Figure S7 shows the enthalpy of formation, H_f, for all Mo-Si crystal structures, present in the training (yellow squares) and testing (blue squares) datasets. The vdW-DF-CX data (red triangles) is given for comparison. The H_f is computed using Eq.(2).

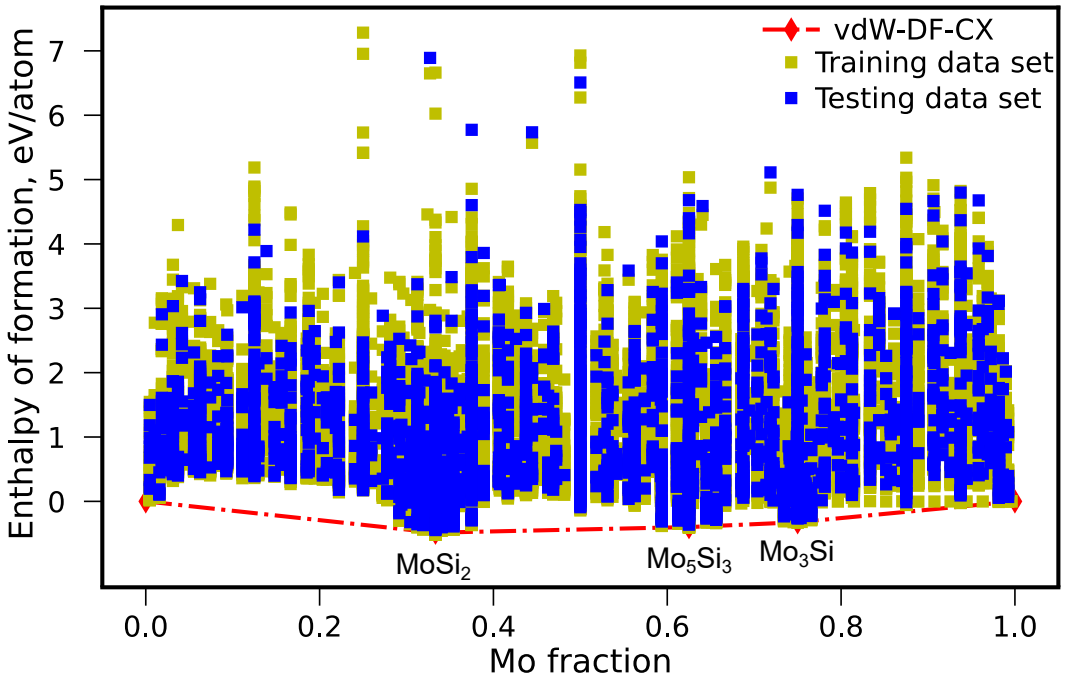

Figure S7: Formation enthalpy, computed for all Mo-Si crystal structures, present in the training (yellow squares) and testing (blue squares) datasets. The vdW-DF-CX data (red triangles) is given for comparison.

4 Phonon dispersion

Figure S8 displays phonon band structures for the Mo-Si phases located on the convex hull. Calculations are performed using the ACE potential in conjunction with the `phonopy` package [5]. All three phases are mechanically stable as documented by the absence of imaginary frequencies.

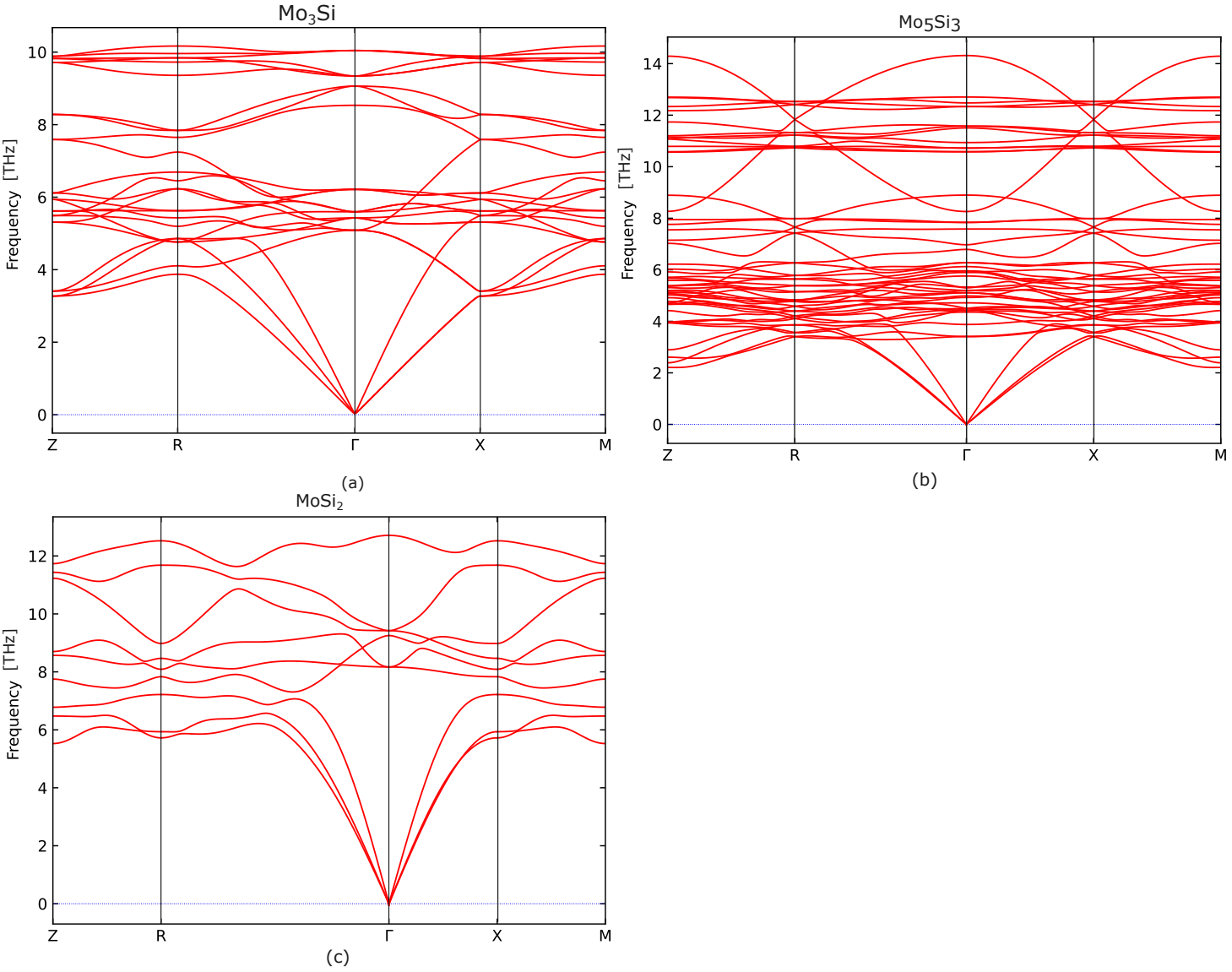

Figure S8: Phonon dispersion along the high symmetry lines in the Brillouin Zone for (a) Mo_3Si, (b) Mo_5Si_3 and (c) $MoSi_2$ phases.

38

5 Elastic constants of Mo, Si and Mo-Si compounds

Mo				
Elastic constants	Experiment	Mo-Si ACE	vdW-DF-CX	MEAM [6]
C11	470 GPa	451 GPa	477 GPa	460 GPa
C12	168 GPa	176 GPa	163 GPa	168 GPa
C44	107 GPa	112 GPa	110 GPa	111 GPa
Si				
Elastic constants	Experiment	Mo-Si ACE	vdW-DF-CX	MEAM [6]
C11	166 GPa	122 GPa	153 GPa	162 GPa
C12	64 GPa	59 GPa	60 GPa	65 GPa
C44	80 GPa	60 GPa	73 GPa	73 GPa
Mo_3Si				
Elastic constants	Experiment	Mo-Si ACE	vdW-DF-CX	MEAM [6]
C11	449 GPa	489 GPa	477 GPa	641 GPa
C12	137 GPa	131 GPa	143 GPa	63 GPa
C44	113 GPa	104 GPa	115 GPa	404 GPa
Mo_5Si_3				
Elastic constants	Experiment	Mo-Si ACE	vdW-DF-CX	MEAM [6]
C11	446 GPa	418 GPa	444 GPa	326 GPa
C33	390 GPa	353 GPa	410 GPa	448 GPa
C12	174 GPa	164 GPa	170 GPa	141 GPa
C13	140 GPa	143 GPa	142 GPa	134 GPa
C44	110 GPa	92 GPa	111 GPa	110 GPa
C66	140 GPa	128 GPa	141 GPa	153 GPa
$MoSi_2$				
Elastic constants	Experiment	Mo-Si ACE	vdW-DF-CX	MEAM [6]
C11	417 GPa	383 GPa	389 GPa	252 GPa
C33	515 GPa	498 GPa	489 GPa	510 GPa
C12	104 GPa	118 GPa	114 GPa	145 GPa
C13	84 GPa	72 GPa	90 GPa	148 GPa
C44	204 GPa	167 GPa	194 GPa	26 GPa
C66	194 GPa	191 GPa	190 GPa	75 GPa

Table S5: Elastic constants of the crystalline Mo, Si and Mo-Si phases, computed using ACE Mo-Si potential, vdW-DF-CX functional and MEAM potential, developed by Baskes [6].

6 Loss function

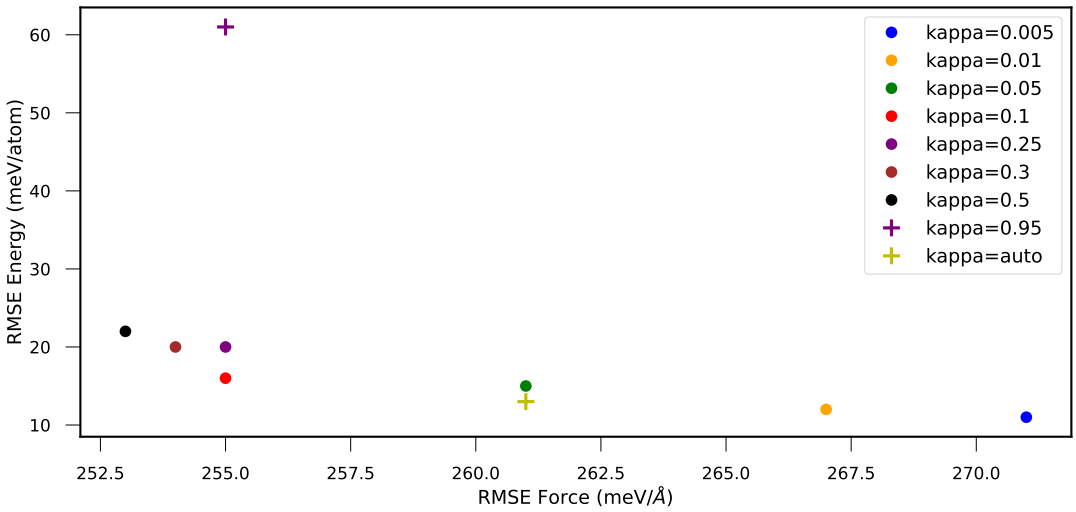

Figure S9: The RMSEs for energy and forces, defined for different values of the loss function, used for training of the ACE Mo-Si potential.

The distribution (standard deviation) of the training energies and forces in the loss function has to be balanced. Figure S9 shows the root-mean-square errors (RMSEs) for energies and forces for the training dataset, defined for different values of the loss function, specified during the training of the ACE Mo-Si potential.

References

[1] A. Misra, J. Petrovic, T. Mitchell, *Scripta Mater.* **1998**, *40*, 2 191.

[2] K. Kishida, Z. Chen, H. Matsunoshita, T. Maruyama, T. Fukuyama, Y. Sasai, H. Inui, M. Heilmaier, *Inter. J. Plasticity* **2022**, *155* 103339.

[3] M. Azim, H.-J. Christ, B. Gorr, T. Kowald, O. Lenchuk, K. Albe, M. Heilmaier, *Acta Mater.* **2017**, *132* 25.

[4] M. Milosavljević, U. Burkhardt, P. Moll, M. König, H. Borrmann, Y. Grin, *Chemistry – A European Journal* **2021**, *27*, 57 14209.

[5] A. Togo, *J. Phys. Soc. Jpn.* **2023**, *92*, 1 012001.

[6] M. Baskes, *Mater. Sci. Eng., A* **1999**, *261* 165.